ENCLOSURE 2

MFN 16-072

Response to Round 5 Requests for Additional Information 103 and 104, 65 (Revised), and 33 (Revised)

Non-Proprietary Information – Class I (Public)

IMPORTANT NOTICE

This is a non-proprietary version of Enclosure 1, from which the proprietary information has been removed. Portions of the enclosure that have been removed are indicated by an open and closed bracket as shown here [[ ]].

RAI 33

Please provide the following information related to PIRT item C18 (cladding perforation):

a. A summary of or reference for the tests that includes the number of tests, the type(s) of cladding tested, and the heatup rates used.

b. The basis for applying the empirical data used to estimate clad rupture stresses to current-generation fuels.

c. The basis for the assumption of normality for the upper and lower 95 percent groups used to determine the rupture stress.

d. Explanation of the origin of and justification for the assumed uncertainty of the built-in fuel rod internal pressure curves and the normality of the multiplier on rod pressure.

e. Relative to the high-temperature phase change of zirconium, please clarify the statement on page 2-11 of the TR that phase change of in-core materials is not modeled.

RAI 33 Response (Revised)

a. A summary of the cladding hoop stress versus perforation temperature testing used in defining the model and model uncertainty can be found in Reference R33-1. The figures in the referenced letter's enclosed report show the comparison of high temperature test data to the rupture stress model. All of the tests presented are for heat-up rates [[

]]. In Reference R33-1 selected data from Reference R33-2 is compared with GE proprietary data for low heat-up rates. Note that ruptures occur at lower hoop stresses when the heat-up rates are lower so that is why the data for the higher heat-up rates in Reference R33-2 are not included. Figure 5 of Reference R33-1 aggregates data points from Figures 1, 2, and 4 of the same reference. Figure R33-1 of this response has been reconstructed from the same data in order to provide a legend to indicate the origins of the data. The relevant NUREG-0630 (Reference R33-2) data that has heat rates of [[ ]] are also depicted with open blue markers in Figure R33-1. [[

]]

b. The clad rupture stress model is assessed using hoop stresses, as described by the method in Section 3.1 of Reference R33-2. By employing this method of converting differential pressure data to hoop stress data, design-specific dimensional effects are eliminated. This allows the clad rupture stress model to be extended beyond the 7x7 and 8x8 fuel from the test programs to current-generation fuel product lines. Additionally, the data in Figure 1 of Reference R33-1 show that the differences between 7x7 and 8x8 fuel rod data extracted from NEDM-20350-3 are insignificant compared to the scatter in the data, confirming that dimensional effects

have been eliminated. This fact is also depicted by comparison of the red triangles (8x8) with the red squares (7x7) in Figure R33-1 of this response.

c. The clad rupture stress uncertainty model was developed using temperature-dependent rupture stress data from GE material testing programs. Relevant low heat-up rate data from NUREG-0630 has been shown for comparison. The uncertainty model [[

]]

d. The LHGR- and exposure-dependent values of the nominal fuel rod internal pressure used in TRACG LOCA analyses are calculated based on the NRC-approved PRIME model [[ ]] The calculation method qualified previously for GESTR (Reference R33-3) has been replaced by PRIME thermal-mechanical analyses (References R33-4 and R33-5). [[ ]] The key driver of rod perforation uncertainty is the uncertainty in the temperature-dependent rupture stress. The rod internal pressure is less important. PRIME nominal rod internal pressure as used in LOCA calculations is [[ ]] shown in Figure 5.2 of Reference R33-5. Updated data provided in Figure 2-8 of Reference R33-6 are replicated here as Figure R33-3. [[

]]

e. Clarifications to the entries in Columns 2 and 3 in Section 3.3.2 of Table 2.5-1 on page 2-11 of the TR are proposed in view of the additional details and clarification provided below.

The entry in column 2 labeled *GEH Process* will be modified to read:

> Material properties for Zircaloy account for the alpha and beta phases. The Zr-H2O reaction to produce ZrO_2 is modeled. Melting of UO_2 is precluded by the GE SAFDL applied for AOO transients and this bounds all LOCA calculations provided the 2,200 °F limit on PCT is satisfied. Eutectic formations are not significant provided the 2,200 °F limit on PCT is satisfied.

The entry in column 3 under *Evaluation* will be modified to read:

> The phenomena necessary for BWR LOCA are modeled.

Cladding hoop stresses are modeled in TRACG for the purpose of tracking geometric changes due to rod perforation and to account for the resulting oxidation of the cladding. Additionally, material properties for the cladding and fuel take into account transient temperature effects. Specifically, the Zircaloy cladding properties account for the physical differences associated with the alpha and beta phases of Zircaloy. The contact pressure between the UO2 pellet and cladding inside surface is specifically modeled and is strongly influenced by uncertainty in parameters that impact the temperature of the fuel pellet and its thermal expansion. If the 10 CFR 50.46(b) acceptance criteria for ECCS systems are met, the chemical effects of eutectic formation will have no adverse impact on the fuel and can be ignored in cladding response calculations within the range of post-LOCA conditions. Proposed additional requirements from 10 CFR 50.46(c) related to post-quench ductility and break away oxidation are expected to be addressed by material testing that will be used to stipulate a time limit at a prescribed temperature that must not be exceeded in the LOCA calculations. Assessment relative to the new criteria is independent of the TRACG modeling and application methodology and can be achieved by comparing the calculated PCT trace to the required limit once the new rules are finalized.

[[

]]

Figure R33-1. Rupture Stress Model Compared to Data

[[

]]

Figure R33-2. Examples of Rupture Stress Uncertainty Modeling

[[

]]

Figure R33-3. PRIME Predicted versus Measured Fuel Rod Internal Pressure (Nominal)

References

R33-1. Letter from R. W. Bucholz (GE) to C. S. Rubenstein (NRC), "General Electric Fuel Clad Swelling and Rupture Model," MFN-097-81, May 15, 1981.

R33-2. NUREG-0630, Cladding Swelling and Rupture Models for LOCA Analysis, April 1980.

R33-3. B.S. Shiralkar, et al. "The GESTR-LOCA and SAFER Models for the Evaluation fo the Loss-of-Coolant Accident, Volume I: GESTR-LOCA – A Model for the Prediction of Fuel Rod Thermal Performance," NEDE-23785-1-PA, Revision 1, October 1984.

R33-4. "The PRIME Model for Analysis of Fuel Rod Thermal-Mechanical Performance Part 3 – Application Methodology," NEDC-33258P-A, Revision 1, September 2010.

R33-5. "The PRIME Model for Analysis of Fuel Rod Thermal-Mechanical Performance Part 2 – Qualification," NEDC-33257P-A, Revision 1, September 2010.

R33-6. "The PRIME Model for Analysis of Fuel Rod Thermal-Mechanical Performance 2015 5-Year Update", NEDC-33257P Supplement 1, MFN 15-060, August 7, 2015.

LTR Impact

Entries in Columns 2 and 3 in Section 3.3.2 of Table 2.5-1 on page 2-11 of the TR will be revised.

The entry in Column 2 labeled *GEH Process* will be modified to read:

> Material properties for Zircaloy account for the alpha and beta phases. The Zr-H2O reaction to produce ZrO_2 is modeled. Melting of UO_2 is precluded by the GE SAFDL applied for AOO transients and this bounds all LOCA calculations provided the 2,200 °F limit on PCT is satisfied. Eutectic formations are not significant provided the 2,200 °F limit on PCT is satisfied.

The entry in Column 3 under *Evaluation* will be modified to read:

> The phenomena necessary for BWR LOCA are modeled.

LTR Section 5.1.3.24 will be replaced to read as indicated below. The figure titled "Uncertainty in Fuel Rod Internal Pressure" in the LTR as originally submitted will be deleted. The figure titled "Clad Rupture Stress as a Function of Clad Temperature" in the LTR as originally submitted will be replaced using Figure R33-1 from this response.

5.1.3.24 C18 – Fuel Cladding Strain /Perforation (H)

The key drivers governing strain-induced fuel rod perforation are the temperature-dependent clad rupture stress and the rod internal pressure. Based on material properties, the rupture stress and its associated uncertainty is modeled in TRACG as three curves corresponding to nominal, lower bound, and upper bound rupture stress curves as functions of cladding temperature (Figure 5.1 15). At each temperature, the upper and lower bounds are used to define uniformly-distributed samples above and below the nominal rupture stress, respectively.

The instantaneous clad hoop stress is directly related to the fuel rod internal pressure. Nominal fuel rod internal pressures are calculated in TRACG as described in Section 7.5.3.1 of Reference [1] using parameters calculated by PRIME [76] and passed to TRACG [[

]]

RAI 65

Section 7.1.1 of the TR states that continuity in the probability density functions for figures of merit is a requirement for determining non-parametric tolerance limits according to Wilks' Theorem. However, it is not obvious that these probability density functions will, in general, be continuous. In fact, [[ ]] calls the TR's assumption of continuity into question. Therefore, please demonstrate that the requirement for continuous probability density functions will be satisfied in the application of the evaluation model described in the TR for quantifying a single probabilistic statement of safety for the complete spectrum of break locations and sizes, the complete spectrum of model parameters and their variation, and the nonlinear feedback introduced by the engineered safety features. In other words, please show that there are no disjoint density functions of the figures of merit, or they can be identified and taken into account in the application of Wilks' Theorem.

RAI 65 Response (Revised)

Continuity of the probability density functions for figures of merit is not a requirement for determining the non-parametric tolerance limits. Although the original work by Wilks is based on continuity of the probability density function, Wald's work further extends the method to multivariate applications (Reference R65-1), and Tukey's work extends the nonparametric estimation technique to discrete distributions (Reference R65-2). As demonstrated in RAI-6 and RAI-9 responses, the bifurcated behavior is effectively eliminated from the computed results. The simulations performed to date support that the probability density functions for figures of merit are practically from continuous functions. The methodology does not depend on a continuity requirement. Therefore, the sentence regarding this aspect being a requirement will be removed.

References

R65-1 A. Wald, "An Extension of Wilks' Method for Setting Tolerance Limits," *The Annals of Mathematical Statistics*, Volume 14, Issue 1, March 1943, 45-55.

R65-2 J. W. Tukey, "Nonparametric Estimation, III. Statistically Equivalent Blocks and Multivariate Tolerance Regions – The Discontinuous Case," *The Annals of Mathematical Statistics*, Volume 19 (1948), pp. 30-39.

LTR Impact:

Following sentence from Section 7.1.1 of the LTR will be removed:

"The only requirement for the validity of the OSUTL derived in this manner is continuity of the PDFs providing the samples for each trial."

RAI 103

In response to prior RAIs 66 and 89, GEH provided justification for its proposed approach of analyzing uncertainty using at least three statistical samples, each containing 59 cases. The NRC staff does not accept the GEH justification that this approach provides the high-probability results required 10 CFR 50.46. In particular, because the method is used to determine high-probability results for three different critical safety parameters, an approach based on order statistics should identify an upper quantile, but should do so with high confidence. The high confidence is required so that the variability associated with using quasi-random samples to infer upper quantiles is either minimized or conservatively taken into account. Thus, in identifying a basis for a specified sample size, consideration of tri-variate coverage and the use of tolerance intervals are considered by the NRC staff to be acceptable approaches. Provide a statistical sampling basis that estimates an upper tolerance limit and provides tri-variate coverage. If the approach is proposed to allow other than the first-ranked order statistic as the upper tolerance limit, please also clearly delineate the approach for setting the sample size and number of rejected order statistics, providing information to demonstrate that sample sizes are set prior to initiation of production statistical analysis.

RAI 103 Response

In RAI-66 response, the GEH position depended solely on the limited discussion provided in RG 1.157 regarding the acceptable ways of quantifying the uncertainty. This position partly stemmed from the following fact: For all fuel types and core designs in BWRs, when the maximum local oxidation (MLO) criterion is met, the hydrogen generation, also referred to as core-wide oxidation (CWO), is always limited to less than 1% of all cladding surrounding the fuel. Therefore, meeting the criterion is not a random outcome, but is a function of the MLO. The guidance provided by the regulatory guide did not place the MLO and CWO acceptance criteria at the same statistical treatment for uncertainty calculation compared to the peak cladding temperature (PCT) criterion. GEH understands that the staff's expectation has evolved, and now it demands the treatment of all three critical safety parameter with the same statistical rigor and reporting on their joint probability with a specified confidence as if they are from dependent distributions with no assumption on their correlation.[1] Since the approach using tri-variate coverage and tolerance intervals is considered acceptable by the NRC staff for quantifying the uncertainties to determine the three different critical safety parameters, GEH will comply with this expectation by adapting a sampling scheme that is purely based on order statistics.

To meet this expectation, it is necessary to adjust the minimum number of samples. The non-parametric statistical theory determines the sample size necessary to establish the statistical argument. In TRACG LOCA methodology, widely-accepted 95/95 criteria will be used. In other words, the joint probability on the reported 95th percentile values reported for the three critical

[1] As shown in Reference R103-1, if the parameters of interest have perfect correlation, the minimum number of samples reduces to the required number for single parameter. In this application, no assumption for the level of correlation will be made, but they are treated as statistically dependent.

safety parameter will be no less than 95%. The first multivariate generalization of Wilks' order statistics work [Reference R103-2] was made by Wald [Reference R103-3]. His method has been termed that of 'successive elimination.' The distribution of the coverage is shown by Wald to be the Beta distribution.

J. W. Tukey generalized the construction of distribution-free tolerance regions for any general shapes, such as rectangles, cubes, polygons, ellipsoids, or spheres, by introducing the concept of statistically equivalent blocks [Reference R103-4]. Using this concept, it is possible to construct a statistical sampling scheme that meets the aforementioned criteria.

Similar to the example given in References R103-1, for three critical safety parameters, or independent figures of merit (FOMs), evaluated at 95% coverage with 95% probability (95/95), the minimum number of cases without any rejection is 124. In other words, the highest ranked output parameters for each FOM, i.e. the maximum values from the 124 cases, will determine the 95/95 peak cladding temperature (PCT), maximum local oxidation (MLO), and core-wide oxidation (CWO). Using the same theory, the second highest value for only one of the critical parameter would be equal or greater than 95% of the true population with 95% confidence level when the sample size is 153. Similarly, with a sample size of 181, it is possible to have 2 samples with highest values for any of the critical safety parameters removed to form the tolerance limits and still satisfy the 95/95 requirement for each of them. Table R103-1 provides the sample size needed to ensure that 95th percentile of a given FOM would be exceeded with 95% probability for various degrees of freedom (DOFs).

Table R103-1 Minimum number of runs for different sampling schemes

	m (DOF-2)	n	# of allowed failures
Scheme A	3	124	0
	4	153	1
Scheme B	5	181	2
	6	208	3

Scheme A as noted in Table R103-1 meets the expectation of 95%/95% coverage for tri-variate sampling with no rejection. Scheme A will be used unless stated otherwise prior to the analyses.

Scheme B sampling provides for a more robust process that is less prone to added conservatism coming from statistical variation in the extreme values by allowing up to two failures from a larger sample size of 181 trials. In this context, the term failure is used for a trial with a FOM output that is beyond the 95% probability for 95% coverage. A trial value might be rejected for exceeding a preset limit such as a regulatory acceptance criterion; however, rejection of two samples with maximum values for any of the FOMs is allowed because two extreme values are beyond the needed 95% probability for 95% coverage when the sample size is 181. Scheme B allows a more accurate evaluation of the critical safety parameters. It will be employed for plant applications where there is a credible expectation that the regulatory limits would be challenged. For instance, BWR/2 applications would fall under this category.

The equivalency of Schemes A and B is demonstrated by the following examples. To simplify the subsequent discussions, the CWO dimension of the results is omitted in the following illustrations since the criterion is always met when the MLO critical safety parameter meets the acceptance criterion, eliminating the need to plot a third dimension in the figure. But, the same concept applies. The red circles and blue diamonds in Figure R103-1 show the MLO values versus PCT values for each of the trials from a 181-case and 124-case statistical analysis of BWR/2 large-break LOCA, respectively. Shown in the figure are the boxes that define the 95% coverage for the joint probability for three tri-variant critical parameters with 95% confidence level.

[[

]]

Figure R103-1 BWR/2 Large Break LOCA Results: MLO versus PCT

Figure R103-1 is constructed using two separate random sets, one with 124 cases (blue diamonds) and the other with 181(red circles). As the number of samples increase, the distribution of the cases in the box would asymptotically converge to the exact 95%. Table R103-2 shows the numerical values for PCT and MLO. CWO is not shown because it is never limiting. The highest CWO value from all trials remaining after any trials are rejected based on PCT and/or MLO will be reported and checked to confirm it is under the regulatory limit.

Table R103-2 Highest calculated PCT and MLO values from 124- and 181-case exercises

[[		
		]]

Furthermore, it is noted that when Scheme B is adapted using 181 samples, the boxes shown in Figure R103-2 are also statistically equivalent to describe the joint probability. Earlier work by Fraser (Reference R103-5) provides evidence that the method still remains valid if the function that determine the statistically equivalent blocks are chosen by a random process from a class of such functions. The point is true for any sequence and consequently is true when the sequence is chosen by a random process (Reference R103-5). Work by Kemperman (Reference R103-6) further generalized the method for constructing tolerance limits by allowing that each step of construction may not only depend on the blocks previously formed, but also on all the known boundary observations, replacing Tukey's lexicographical ordering. Adaptation of generalized tolerance limits using sequentially determined statistically equivalent blocks implies that, when Scheme B is selected with 181 cases, eliminating (1) highest two PCT results, (2) highest two oxidation results, or (3) one of each would be statistically equivalent in evaluating the coverage. In Figure R103-2, both boxes define the 95% coverage with 95% confidence for the joint probability with the third dimension for CWO omitted from the figure as explained above.

[[

]]

Figure R103-2 Statistically Equivalent Blocks for BWR/2 Large Break LOCA Results

In accordance with the principles laid out in RAI-99, the sampling plan will be set at the onset of the analysis and there will be no modification of either the sampling scheme or the unique seed assigned to the analysis for a given plant. However, the commitment regarding the use of tri-variate order statistics overrides the position for analysis sample size given in the RAI-99 response. Similarly, the RAI-66 response is also superseded by the sample size scheme given in this response.

References

R103-1 A. Guba, M. Makai, L. Pál, "Statistical aspects of best estimate method – I," Reliability Engineering and System Safety, Volume 80, (2003) pp. 217–23.

R103-2 S. S. Wilks, "Determination of sample sizes for setting tolerance limits," The Annals of Mathematical Statistics, Volume 12 (1941), pp. 91-96.

R103-3 A. Wald, "An Extension of Wilks` Method for Setting Tolerance Limits," The Annals of Mathematical Statistics, Volume 14 (1943), pp. 45-55.

R103-4 J. W. Tukey, "Nonparametric estimation II: Statistically equivalent blocks and tolerance regions – the continuous case," The Annals of Mathematical Statistics, Volume 18 (1947), pp. 529-539.

R103-5 D. A. S. Fraser, "Sequentially Determined Statistically Equivalent Blocks," The Annals of Mathematical Statistics, Volume 22 (1951), pp. 372-381.

R103-6 J. H. B. Kemperman, "Generalized Tolerance Limits," The Annals of Mathematical Statistics, Volume 27 (1956), pp. 180-186.

LTR Impact

Pertinent parts of Chapter 7 and 9 will be updated. It will be noted in Revision 1, Chapter 8 runs will not be repeated with this change.

The affected Chapter 7 and 9 pages follow.

7.0COMBINATION OF UNCERTAINTIES

A Monte Carlo technique is used to combine the individual biases and uncertainties specified for initial conditions, plant, and model parameters into an overall bias and uncertainty for the LOCA safety criteria. The Monte Carlo sample is developed by performing random perturbations of the parameters over their individual uncertainty ranges. Using the histogram generated by the Monte Carlo sampling technique, a probability density function is generated for the calculated primary safety criteria parameters.

To determine the total uncertainty in computer code predictions, it is necessary to combine the effects of model uncertainties (CSAU Step 9), scaling uncertainties (CSAU Step 10) and plant condition or state uncertainties (CSAU Step 11). Various methods have been used to combine the effects of uncertainties in a safety analysis, which are discussed briefly in [3]. All these approaches are within the framework of the CSAU methodology. This section only describes the methods for combining uncertainties that are proposed to be used for the TRACG ECCS/LOCA application. The method used for combining uncertainties in the application of TRACG to ECCS/LOCA analyses is the same as that used successfully and approved by the NRC for the analyses of AOO transient scenarios [3].

7.1 APPROACHES FOR COMBINING UNCERTAINTIES

Four approaches have been discussed and compared in [3] for combining uncertainties, which are: (1) Propagation of Errors; (2) Response Surface Technique; (3) Order Statistical (OS) Method, and (4) Normal Distribution One-Sided Tolerance Limit. Only the last two approaches will be briefly discussed in the following sections (Sections 7.1.1 and 7.1.2) since a multivariate version of order statistics is adapted for the TRACG ECCS/LOCA application and normal distribution assumption is used in some of the Chapter 8 demonstration calculations.

7.1.1 Order Statistics (OS) Method

In contrast to the Response Surface Technique, the non-parametric sampling method that has been used in Germany by Gesellschaft für Anlagen-und Reaktorsicherheit (GRS) [28] and for the application of TRACG to AOOs by GEH [3] requires only a relatively small number of calculations and automatically includes the effects of interactions between perturbations to different parameters. In the OS method, randomly sampled trials are used to vary all uncertain model and plant parameters randomly and simultaneously, each according to its uncertainty and assumed PDF. A method based on the order statistics of the output values is then used to derive one-sided upper or lower tolerance limits (OSUTLs or OSLTLs). For ECCS/LOCA applications, OSUTLs are defined for primary safety parameters such as the PCT, maximum clad oxide thickness fraction, and maximum zirconium oxide volume fraction.

Random sampling of each model, plant and state parameter according to its assigned PDF yields the value of that parameter to be used for a particular trial. For example, a given trial could have the film boiling heat transfer coefficient set at its -1.5σ value and the interfacial shear set at its +2.0σ value, each according to its own probability model. For each randomly sampled set of

parameters, the calculation process determines the output parameters of interest. In this manner, the effects of interactions between parameters are captured in a single calculation. Once all of the trials have been completed, the desired output parameter (e.g., PCT) is extracted from each of the trials and the set of all values of this parameter is used to construct its OSUTL. Figure 7.1-1 illustrates the process.

TRACG overlay files containing all the perturbed input parameter values are created for each trial. The overlay file is appended to the end of the base transient input file and the TRACG calculation is performed to determine the output parameter value (e.g., PCT) as a function of time for this particular set of inputs. Each repeat of the process defines a sample value of the output parameter of interest for the particular transient under consideration. Similar sample values for other output parameters (e.g., maximum cladding oxidation) can be generated at the same time without additional TRACG calculations.

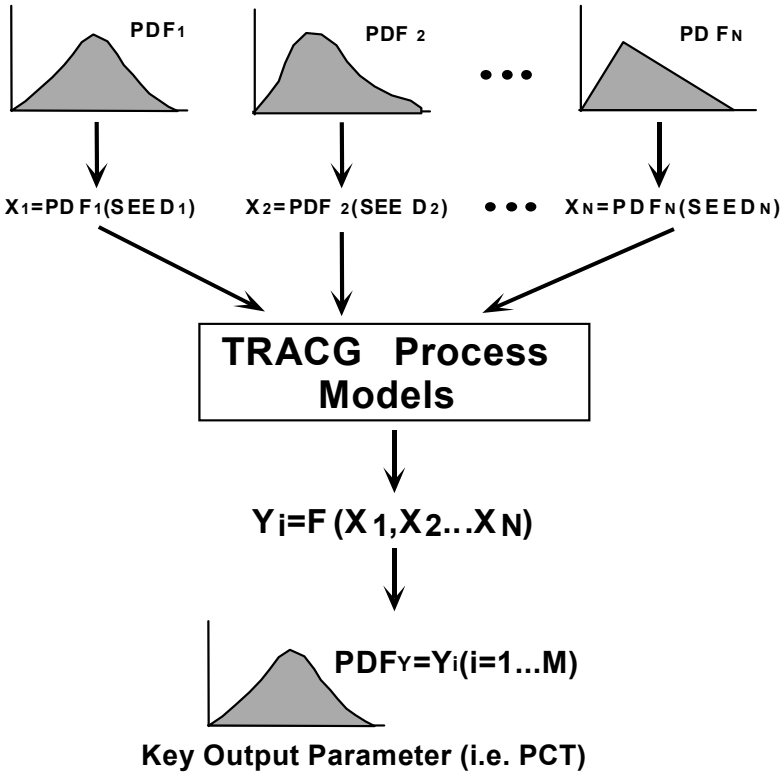

Figure 7.1-1 Schematic Process for Combining Uncertainties

The OSUTL of an output parameter, derived from the results of any given number of trials, is defined by two numbers, $0 < \alpha, \beta < 1$. Denoting the OSUTL by U, it can be stated that the percentage of future values of the output parameter (i.e., values determined from subsequent trials) that will be less than U is $100 \cdot \alpha\%$, with a confidence level of at least $100 \cdot \beta\%$. In formal practice, this is called an OSUTL with $100 \cdot \alpha\%$ content and (at least) $100 \cdot \beta\%$ confidence level. The only requirement for the validity of the OSUTL derived in this manner is continuity of the PDFs providing the input

samples for each trial. It has been shown [30] that, for prescribed values of α and β, the OSUTL can be defined for univariate case as the largest of the output parameter values if the sample size, n, satisfies $n \geq \log(1-\beta)/\log\alpha$. Thus to claim the largest value of a set of trials is an OSUTL with 95%-content and 95% confidence level for a single parameter, the minimum sample size is n = 59.

In multivariate case, the minimum sample size for joint probability of three statistically dependent but not necessarily correlated parameters is 124. In other words, the highest value for each of the three critical safety parameters would provide the joint 95% tolerance limit with 95% probability from a population of 124 cases.

The order statistics method is generally applicable without regard to the underlying probability distribution of the output parameter of interest. It requires only that the individual trials be independent realizations of a random variable from some single probability distribution. For a given number of trials, the upper bound value of the output parameter is itself a random quantity with a variability that depends on the sample size. The variability can be substantial and, on occasion, will yield an overly conservative bound.

To reduce this variability, a larger sample size can be used so that the 95%-content/95% confidence bound is given by the second or third largest observation. In a sample of 124, for example, the largest observation provides the desired bound for trivariate case. It is also possible to increase the sample size to 181 and sequentially eliminate 2 of the samples having the highest values from the population when determining the 95% tolerance limit with 95% confidence.

7.1.2 Normal Distribution One-Sided Upper Tolerance Limit

A special case of the order statistics method arises when the data that the tolerance bound will be derived from can reasonably be regarded as a sample from a normal probability distribution. In this case, it can be shown that the normal distribution one-sided upper tolerance limit (ND-OSUTL) is of the form

$$ND - OSUTL_{\alpha,\beta} \equiv \bar{y} + z_{\alpha,\beta} \cdot s \tag{7-1}$$

where $\bar{y}$ is the average of the outcomes of the trials, s is their standard deviation and the factor $z_{\alpha,\beta}$ is chosen to guarantee 100α%-content with a 100β% confidence level. The assumption of normality for the response data is typically justified via one or more goodness-of-fit tests (e.g., Ryan-Joiner, Shapiro-Wilk, or Anderson-Darling). The values of $z_{\alpha,\beta}$ are tabulated in many statistical textbooks (e.g., [31]) as *factors for one-sided normal tolerance limits*. For example, to establish a bound of 95% content with a 95% confidence level from a sample of 59 trials, $z_{95,95} = 2.024$. As the sample size increases, this factor approaches 1.645, the 95th percentile of the standard normal distribution. If the normality tests indicate that the data are unlikely to have originated from a normal population, the order statistics method should be used. [[

]]

9.0METHODOLOGY APPLICATION

This section provides additional discussion on some of the methodology application aspects. These discussions are to clarify the intended use of the evaluation methodology in analyses.

9.1 ANALYSIS PROCESS SUMMARY

In this report, demonstration analyses are presented along with additional sensitivity studies that helped in making the methodology decisions. The demonstration cases are illustrative and do not represent any particular plant. Actual analysis of a given plant will employ plant-specific input modeling and plant-specific break spectrum calculation. The uncertainty analysis and post-processing of results are built on break spectrum studies. The overall analysis process can be depicted by the flowchart given in Figure 9.1-1.

The process begins with preparation of the plant-specific basedeck. Major inputs to this step are plant geometry data from the qualified database, plant licensing operating parameters for LOCA/ECCS performance evaluation, analysis initial conditions, fuel-specific TRACG channel model, and fuel performance data.

The next major step in the analysis process is the break spectrum studies. The primary goal of this step is to determine the limiting break for further uncertainty analysis. The break spectrum studies are primarily centered on the recirculation line breaks for external pump and jet pump type plants. The appropriate single failure assumption depending on the break analyzed is applied. Additional studies are carried out, if needed, to verify that no other single failure, break location and size, and combination of uncertainty contributors will result in a higher PCT than the limiting break case.

The purpose of the uncertainty analysis, the following step, is to quantify the uncertainties associated with the analysis. For jet pump plant LOCA analysis, [[

]] For the external pump plant LOCA analysis, [[

]] The break spectrum studies combined with sensitivities to the uncertainty contributors presented in this LTR indicate that intermediate breaks are more limiting for jet pump design, whereas the double-ended guillotine is the limiting case for external pump design plants. Although the limiting break size is expected to differ on a plant-specific basis, the overall trends in break spectrum are expected to be similar for the similar designs. Each LOCA analysis will include plant-specific break spectrum calculations.

The statistical analysis of uncertainty quantification relies on well-established techniques. [[

]]

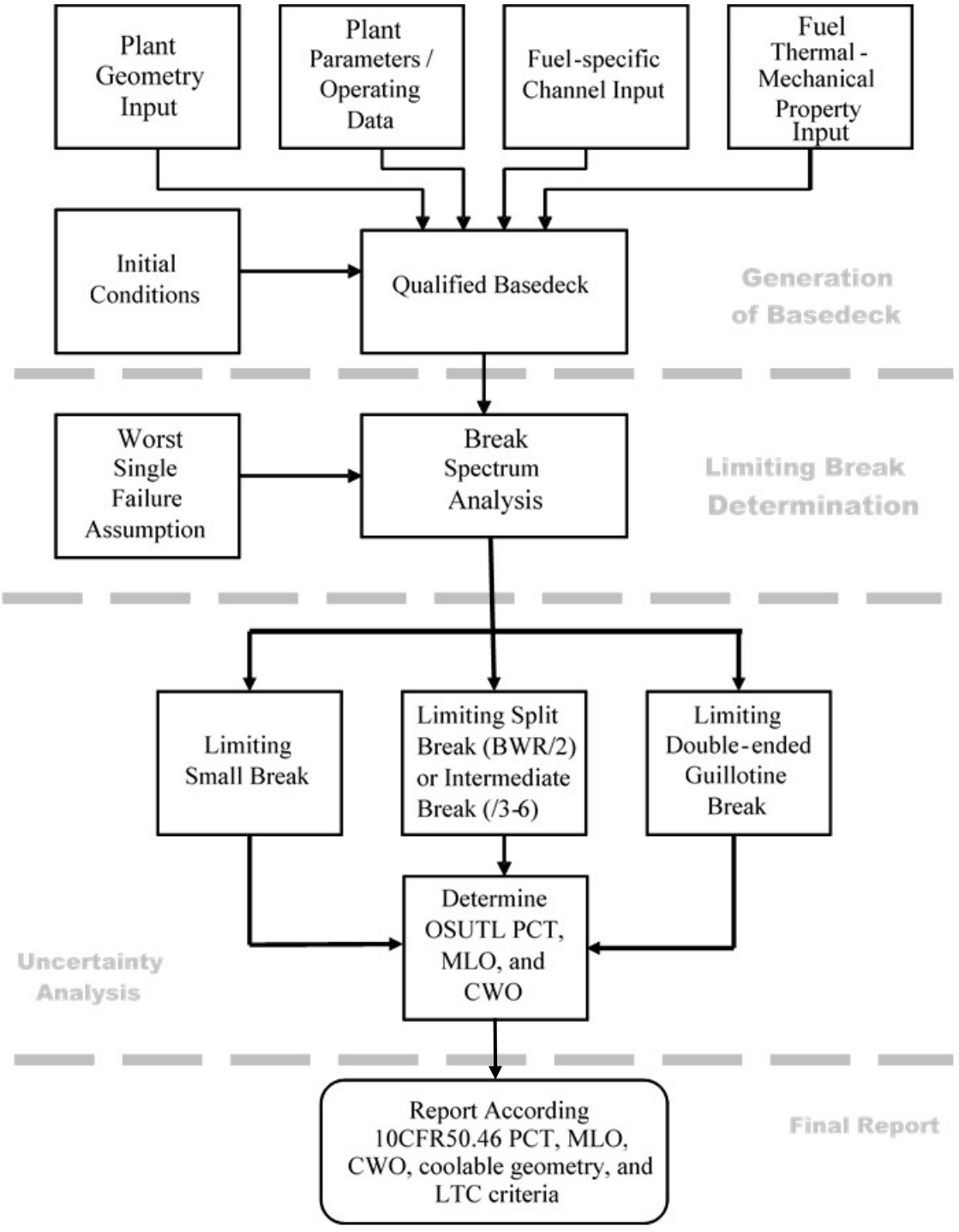

Figure 9.1-1 LOCA Analysis Process Flowchart

RAI 104

Provide additional information to justify the TRACG-LOCA modeling of rewet phenomena. In particular, show the sensitivity of the PCT and ECR to variations in the Shumway correlation-predicted rewet temperature and to variations in the uncertainty associated with the quench front model. Include discussion of limiting BWR transients as well as to appropriate integral effects test.

RAI 104 Response

Summary

Table R104-4 summarizes the additional sensitivity studies performed to assess the impact of the bias and uncertainty applied to the Shumway correlation treatment of minimum stable film boiling temperature (Tmin) and the impact of the bias and uncertainty in the TRACG quench modeling. These sensitivities results provide context for the treatment of Tmin and quench using the proposed best-estimate plus uncertainty (BEPU) approach and should not be viewed as suggesting an alternate analysis approach. The text that follows provides contextual and historical background as well the qualification basis for the Tmin and quench models. Also there is a description of how the requested sensitivity studies were performed and how those results together with previously supplied information justify the TRACG proposed BEPU approach. Additional conservatism is not warranted because the BEPU modeling described in the TRACG LOCA LTR already accounts for bias and uncertainty in the modeling of Tmin and quench in a way that satisfies the regulatory requirements and guidance.

Background

In the response to RAI-98, Reference R98-3 was a citation to MFN 15-078. For convenience Reference R98-3 is cited again here as Reference [R104- 1]. (Citations needed in this document are repeated so the reader is not inconvenienced with tracking down cascading references.) The enclosures to MFN 15-078 contain much information that is relevant to the TRACG models for Tmin and quench. A roadmap to the contents of MFN 15-078 was provided informally to the NRC to facilitate their review and use of the supporting materials in MFN 15-078. Information from the roadmap to the MFN 15-078 enclosures will not be repeated here because information from those enclosures that are especially relevant for LOCA applications and qualification will be cited directly and specific elements will be gathered into this response for the convenience of the reader.

The TRACG implementation of the Tmin correlation and the quench model have been extensively reviewed by the NRC staff and ACRS in association with TRACG ATWSI applications. NRC staff audits on the subject are indicated in Table R104-1 below. Interactions with the ACRS on these subjects are indicated in Table R104-2. The lists in Table R104-1 and Table R104-2 may not include all occurrences. The key point is that the NRC staff and the ACRS have repeatedly requested and scrutinized information on the subjects of Tmin and quench largely in connection

with ATWSI applications where the importance of these model is greater than it is for LOCA applications.

Table R104-1 NRC Staff Audits Where TRACG Tmin and Quench Models were Assessed

Audit Dates	Context of the Audit
October 24-25, 2012	NRC TRACG Tmin and Quenching Methodology Audit MFN 13-073 and MFN 13-085 were produced following this audit so that they could be referenced for customer LARs requiring TRACG ATWSI application to support MELLLA+.
April 23-25, 2014	In connection with MELLLA+ LAR for Grand Gulf submitted by Entergy (see ADAMS Accession No. ML13269A140)
August 31, 2015	In connection with MELLLA+ LAR for Peach Bottom submitted by Exelon. MFN 15-078 was produced to provide documentation requested during this audit.

Table R104-2 ACRS Interactions Where TRACG Tmin and Quench Models were Discussed

Date	Context of the Discussion
November 21, 2013	Presentation to the ACRS on TRACG modeling of Tmin and quench.
March 17, 2015	In support of MELLLA+ for Grand Gulf
May 7, 2015	In support of MELLLA+ for Grand Gulf
July 8, 2015	In support of MELLLA+ for NMP2
September 21, 2015	Presented a simplified version of the materials contained in MFN 15-078.

With respect to TRACG LOCA applications, the biases and uncertainties for both the Tmin and quench models are treated following the best-estimate plus uncertainty (BEPU) approach. The TRACG LOCA modeling conforms with the Code Scaling and Applicability, and Uncertainty (CSAU) methodology described in NUREG/CR-5249 and the guidance provided in Regulatory Guide 1.157. The modeling and bias for the Shumway Tmin correlation are described in Section 5.1.3.26 of the LTR. For the quench model the basis for the bias and uncertainty are presented in Section 5.1.3.27 of the LTR. The descriptions in the LTR are augmented by responses to the RAIs as indicated in the following paragraph.

The responses to RAIs 23 and 50 provide additional information related to the modeling of Tmin. The response to RAI 49 provides additional information related to the modeling of bias and uncertainty for the quench model. A distinction is made in the RAI 49 response regarding the low importance of quench modeling for jet pump BWRs/3-6 compared to the high importance of quench modeling for the BWR/2. As explained in the response to RAI-51: "For jet pump plants, rewet occurs after reflood and the temperature has turned around and starts to come down. The uncertainty in the rewet has therefore no impact on the PCT. Likewise the impact on the fuel clad oxidization for jet pump plants is also minimal as the PCT is relatively low and the duration of refill/reflood phase is short." The Core Spray Heat Transfer (CSHT) tests provide the essential qualification for quenching due to a falling film like in a BWR/2. That is the reason that Monte Carlo analyses of select CSHT tests were provided in Section 7.4.5 of the LTR. The text and figures in Section 7.4.5 have been updated and augmented in response to RAI 92.

To respond to the specific NRC request in this document, sensitivity studies have been performed to justify the current treatment of bias and uncertainty for both the Modified Shumway (MS) correlation for minimum stable film temperature (Tmin) and the quench model. ("Modified Shumway" refers to the Shumway correlation with the elimination of the enhancement due to lower void fractions as explained later.) ALL sensitivity studies have been performed using 181 statistical trials and the limiting case for the NMP1 BWR/2 LOCA analysis. Use of the NMP1 BWR/2 calculations for the sensitivity studies is the most appropriate because the time in boiling transition for a BWR/2 is substantially longer than for BWRs/3-6 LOCA evaluations. For the limiting BWR/2 LOCA scenario only core spray is available to cool the core; consequently, rewetting occurs much later and the impact of any process that delays rewetting has the largest impact on oxide accumulation. By contrast, the cores in jet pump BWRs/3-6 can be re-flooded by the ECCS systems at least to the top of the jet pump diffusers within a comparatively shorter period of time so that total oxide accumulation remains much less than the imposed regulatory limit of 13% for cladding maximum local oxidation (MLO). It is also true that BWR/2 LOCA calculations tend to provide a higher calculated peak clad temperature (PCT) relative to BWRs/3-6 evaluated for the same or even higher linear heat generation rates (LHGRs).

For both the Tmin and quench, the requested additional sensitivity studies are performed by setting the associated PIRT multiplier at its de-biased value minus two standard deviations (sigma). The specific bias and uncertainty values are those indicated in the TRACG LOCA LTR and supported by responses to a number of different RAIs. Details that are presented below justify the proposed TRACG BEPU approach modeling of bias and uncertainty for the Tmin and quench models for LOCA applications. To the greatest extent possible, the technically sound models implemented in TRACG are supported by comparing calculated results to relevant test data.

Justification of TRACG Tmin Modeling

Detailed information on Shumway's correlation for Tmin is available in MFN 13-073 cited as Reference R50-1 in the response to RAI-50 and repeated in this document as [R104- 2]. Section 5.1.3.26 of the TRACG LOCA LTR has been modified as described in the RAI-50 response and the reference to MFN 13-073 added as Reference 80 in Section 11. The equation for the Shumway correlation is given in MFN 13-073 and also by Equation (6.6-52) of the TRACG Model LTR (cited as Reference 1 in the TRACG LOCA LTR and repeated here as [R104- 3]). The equation origin is Equation (19) in EGG-RST-6781 which is cited as Reference 3 in [R104- 2], Reference 23 in [R104- 3], and directly cited here as [R104- 4]. The primary purpose of MFN 13-073 was to justify using the Shumway correlation to calculate Tmin for Zircaloy cladding. Key elements relevant to this justification are gathered from the sources listed above and are assembled here. The specific focus here is on TRACG LOCA applications even though most of the justification is generic for any applications where Tmin is important.

Shumway correlated the *quench temperature* (T_Q) and has done so with the intention that his correlation be implemented in the boiling water reactor (BWR) version of TRAC (TRAC-B). Shumway makes the point that a computer code like TRAC-B (also TRACG) does not need the so-called true Tmin value corresponding to the location on the boiling curve where the heat flux is minimum (Q_{min}). Instead TRAC-B (and TRACG) need a higher Tmin value consistent with

how the heat flux for transition boiling is interpolated between a film boiling heat flux (Q_{FB}) and the critical heat flux (Q_{CHF}). All Shumway's statement for TRAC-B applied also to TRACG. As implemented in TRACG and explained in the response to RAI-069, the value for Tmin is used as a logical check to prevent transition to nucleate boiling when the calculated cladding surface temperature is above Tmin. The main point is that what the computer code needs is to define the temperature below which transition boiling can occur and the heat transfer coefficient will start increasing. Shumway defines the quench temperature (T_Q) to be the temperature of the surface at which significant deviations from film boiling are observed from a temperature versus time or distance curve. In other words, at T_Q there is an observable increase in the rate that the surface temperature is dropping that implies that the heat transfer coefficient is increasing. Carbajo (Reference 2 in [R104- 2]) equates the *quench temperature* with the *rewetting temperature* at which liquid can reestablish (and maintain) contact with the dry surface. By GEH's definition, this would be the *minimum stable film boiling temperature* (Tmin) or the cladding surface temperature below which stable film boiling can no longer be maintained.

As Shumway states, the shape of the boiling curve is influenced by many phenomena which change in importance with the varying experimental conditions. The minimum heat flux (Q_{min}) and the temperature at which it occurs is not exclusively dependent on hydrodynamic or thermodynamic properties of the fluid. It varies with surface conditions such as roughness and surface thermodynamic properties. Factors such as velocity, pressure, subcooling, drop size, liquid contact angle, wetting agents, and even gravity influence the minimum heat flux. In fact, at higher mass fluxes the minimum conditions may not exist. The existence or nonexistence of a Tmin point could be of little consequence provided the computer code implementation provides a reasonable heat transfer coefficient for modeling the transition between stable film boiling and nucleate boiling. In Shumway's words, "Tmin is not a natural or physical property but is a consequence of many competing processes".

Shumway's correlation was established exclusively from **s**tainless **s**teel (SS) data over a relative wide range of pressures and flow rates as shown Figure R104-1. The GEH evaluation of the correlation compared to its own SS data is that on average it conservatively overestimates the 81 useable data points by 23 K with a standard deviation of 55 K when evaluated at α=1. Most of the overestimation is at the higher pressures. For pressure at and below 0.7 MPa that are most relevant for LOCA applications, the bias is -1.2 K. As explained in RAI-50, a 20% uncertainty applied to the calculated difference (Tmin-Tsat) sufficiently covers the 55 K standard deviation. In TRACG LOCA applications no credit is taken for the slight conservative bias at low pressure since this bias is not considered in the BEPU sampling. More important is the fact that the Shumway evaluation of (Tmin-Tsat) as implemented in TRACG is even more conservatively biased for Zircaloy and this bias is not credited.

The Shumway correlation was developed using only SS data. Like many correlations for Tmin, the Shumway correlation accounts for the thermal properties of structure and fluid that impact quenching by using a nondimensional group denoted as β; therefore, the correlation is generally expected to be applicable for a wide variety of metals and fluids as discussed more extensively in Reference [R104- 1]. Henry (Reference [R104- 5]) explains that β relates the invariant temperature

that is achieved at the interface between two semi-infinite slabs of constant properties at different uniform temperatures when they are brought into intimate contact. The ability of β to account for material property differences was assessed by Henry in Figure 9 of his paper cited here as [R104-5]. Figure 4 from [R104- 2] was created to be similar to Henry's Figure 9 with the addition of data from other authors as explained in the text of [R104- 2]. The augmented Figure 4 from [R104- 2] is replicated here as Figure R104-2. The solid symbols in Figure R104-2 were calculated from the Shumway correlation and follow the same color coding used for the other materials. Notice that Shumway's correlation predicts that the (Tmin-Tsat) values for SS304, SS316, and Inconel are very similar due to the fact that the thermal properties, and hence β, for these materials are very similar. As expected from the higher value for β, the Shumway (Tmin-Tsat) value for Zr is also higher. Notice how the Shumway prediction for these low pressures is in the middle of the Zr data from Peterson and Bajorek (Reference [R104- 6]). As shown in Figure R104-2, the Shumway correlation matches overall the trend in both the data and the correlation from Henry over a wide range of material thermal properties. In the range of most interest for SS, Inconel and Zr, the Shumway correlation agrees with both Henry's correlation and the low pressure data within the estimated scatter of the data. Thus the common practice accepted in the industry for over 30 years whereby β is used to account for differences in material properties is justified on a theoretical basis and more importantly supported by comparison with data.

For purposes of comparison, the Shumway correlation used in TRACG and the Groeneveld-Stewart (GS) correlation (Reference [R104- 7]) used in TRACE are shown together as a function of fluid pressure in Figure 5 of [R104- 2] which has been replicated here as Figure R104-3. The GS correlation (depicted by dashed green line) is a simple empirical fit versus only pressure that was developed using only Inconel data and does not include any effect due to different material properties. In the vicinity of the quench location TRACE uses the maximum of Tmin from the GS correlation and 725 K which is shown as dotted black line in Figure R104-3. The solid green curve in Figure R104-3 was obtained from Shumway's correlation using Inconel 600 material properties and the solid purple curve using SS316 material properties. Both evaluations of Shumway's correlation assume no credit for the void fraction term or the Reynolds term in the correlation. As expected, the Inconel and SS curves from Shumway are similar. The purple stars represent T_Q data for SS used by Shumway. The vertical scatter in the data reflects the range of Reynolds numbers for different flow rates as well as other factors such as differences in experimental techniques, geometry, and surface finish. All the open green symbols are for Inconel data extracted from Reference [R104- 8]. The solid green boxes with embedded purple "+" signs were determined from measured T_Q values for SS data in Oak Ridge National Laboratory Thermal-Hydraulic Test Facility (THTF) and Inconel data in Two-Loop Test Apparatus (TLTA) and Rig of Safety Assessment (ROSA)-III Loss-of-Coolant Accident (LOCA) integral system tests that were simulated as part of the TRACG qualification[R104- 9]. The data in Figure R104-3 is widely scattered but this scatter is accounted for in TRACG LOCA applications by consideration of a ±60% uncertainty span in (Tmin-Tsat) that results from the ±3σ sampling where σ=20%.

In Figure 6 of Reference [R104- 2], the Shumway correlation was compared to an additional 894 Inconel data points from the Rod Bundle Heat Transfer (RBHT) tests[R104- 10] as well as integral

LOCA test data. Figure 6 of Reference [R104- 2] is replicated here as Figure R104-4. The RBHT and LOCA integral system tests evaluate quench temperature (T_Q) data consistent with the type of correlation that Shumway developed. To further support use of the Shumway correlation to Zircaloy where Tmin is higher compared to Inconel because of the larger β term, the correlation using Zircaloy has been compared directly to Zircaloy data in Figure R104-4.

The solid red curve obtained from the Shumway correlation as implemented in TRACG using Zircaloy material properties is below the Zircaloy T_Q values extracted from References [R104- 11], [R104- 12], [R104- 13], and [R104- 14] and thus it is conservative for the intended LOCA applications of the TRACG code even without consideration of the uncertainties. There are several plausible explanations for why the Shumway correlation is conservatively low but the most important is that the correlation (solid red curve) was also evaluated assuming that $\alpha = 1$ so no credit would be realized from the term $\left[1+(1-\alpha)^2\right]$ in the correlation. This term has been judged to have inadequate experimental support because in Shumway's words it is based on "a small amount of unpublished Semiscale void data" and the "accuracy of the void effect is untested". Especially for the cases of the Hofmann and Halden data the quench occurs for a much lower void fraction than 1.0 just based on how the liquid water was forced into the test section. It is also likely that a credit for liquid subcooling is observed in the data that is not represented in the Shumway correlation. As an upper bound on the temperature prediction from the Shumway correlation, a value of $\alpha = 0$ was assumed to obtain the dashed red curve in Figure R104-4. The dashed curve is in reasonable agreement with the quench temperature data; however, in applications of the Shumway correlation in TRACG analyses the term $\left[1+(1-\alpha)^2\right]$ is replaced by 1.0 because of the inadequate experimental support for this term.

The Hofmann data contained different amounts of measured oxide although there is so much scatter in the data that the effect on the experimental quench temperatures cannot be discerned. The fuel rods from the GEAP-13112 tests also ended up with a maximum ZrO_2 thickness stated as 1.8 mils considering the measurement uncertainty but unfortunately the amount of oxide was not measured and reported for each TC location. There is no indication in the Halden reports how much oxide accumulated during the tests, but based on the high temperatures and the sustained time at these temperatures, it is likely to not have been negligible. The key point is that the presence of zirconium oxide causes the quench temperatures to increase. Exactly how much the increase should be is debatable. As a basis for comparison, the Shumway prediction of the quench temperature for ZrO_2 is shown (without any credit due to void) by the solid black curve in Figure R104-4. This curve is also in reasonable agreement with the quench temperature data; nevertheless, TRACG analyses that utilize the Shumway correlation will conservatively not take credit for an increase in the predicted T_Q values due to ZrO_2. In other words, the Shumway correlation will be conservatively evaluated using properties for unoxidized Zircaloy.

Based on the Zircaloy temperature data presented in Figure R104-4 one can conclude that using the Shumway correlation as implemented in TRACG to estimate Tmin for Zircaloy is justified because it provides a value of Tmin that is conservatively lower than most of the data even without consideration of the uncertainties as is done in the BEPU TRACG LOCA

application. Lower values of Tmin are more conservative because they delay the return to nucleate boiling and thus result in higher and more conservative calculated values for the cladding temperature.

An objection raised during NRC review of the TRACG LOCA methodology is that the sensitivity of the PCT and ECO results to modeling of uncertainty in Tmin had not been demonstrated for LOCA applications as it was for ATWSI applications. The additional information provided in Table R104-4 of this response addresses that issue. For ATWSI applications of TRACG, sensitivity studies had previously been performed to cause the TRACG Tmin value from the MS correlation to emulate the TRACE implementation of **G**roeneveld-**S**tewart (GS) correlation at the ATWSI pressure of 6.9 MPa. Document page 299 (PDF page 327) of the TRACE V5.0 Theory Manual (Reference [R104- 8]) indicates that **G**roeneveld-**S**tewart [GS] correlation is reset to the maximum of GS and 725 K within 15 cm of a quench front. In the most important vicinity of the quench front the GS correlation is never applied since 725 K is always higher than what the unaltered GS correlation predicts. Based on text from document page 298 (PDF sheet 326), the 725 K limit is applied to compensate for the fact that the GS correlation consistently under predicts the quench temperature.

The ATWSI sensitivity studies applied [[ ]] to obtain a Tmin value of approximately 725 K (like TRACE) for the ATWSI conditions of pressure around 6.9 MPa and cladding temperatures associated with at power conditions. **For the BWR/2 LOCA conditions a lower pressure in the range of 0.10 to 0.14 MPa is appropriate.** [[

]] Results from a preliminary sensitivity study performed for the limiting large break DBA for NMP1 were shown to the NRC during a teleconference on August 16, 2016 and subsequently sent informally to the NRC as an attachment to an email on August 19th. In regard to Tmin sensitivity results, Table R104-4 presented here contains similar contents as presented previously in two tables in the email attachment. Results in Table R104-4 will be discussed in detail later in this document.

Justification of TRACG Quench Modeling

The quench model used in TRACG is essentially the same as the model used in the CORECOOL code currently used together with SAFER when analyzing BWR/2s. The quench modeling was previously reviewed and approved by the NRC as part of their review of NEDE-30996P-A. The relevant references in the TRACG LOCA LTR are [22] and [25]. NRC acceptance of the quench model is documented in the Safety Evaluation (SE) contained in [R104- 15] which is an attachment to the transmittal letter from NRC to GE cited here as [R104- 16].

The quench front model is well described in [R104- 18]. [[

]] These tendencies should be expected based on how the quench model is implemented. Refer to Equations (6), (7), and (8) in [R104- 18]. [[

]]

[[

]]

The quench model works together with the model for Tmin and other elements of the heat transfer package.

[[

]]

The response to LOCA RAI-49 provides additional information related to how uncertainty for the quench model is addressed in TRACG. [[

]]

The heat transfer coefficient for quenching due to bottom reflooding in TRACG had been retained

from TRAC-P1A and TRAC-BD1 and is based on the paper by Yu, Farmer and Coney cited as reference R49-1 in the RAI-49 response and cited in this response as reference [R104- 17]. As explained in the response to RAI-49, the citation of WCAP-7435 (FLECHT) in Section 6.6.13 of the TRACG Model Description LTR [R104- 3] as the source of the heat transfer equation for reflood is not correct and Equation (6.6-158) of Reference [R104- 3] for bottom flooding heat transfer coefficient is also incorrect. The correct expression for the bottom flooding heat transfer coefficient and a more detailed description of the TRACG quench model is available in MFN 13-085 cited here as Reference [R104- 18] and previously provided together with the response to RAI-49. MFN 13-085 also describes the error that was corrected in the interpretation and TRACG coding of the heat transfer correlation for bottom up quenching. The falling film implementations in TRACG and CORECOOL were not affected since they rely on a different heat transfer correlation that was not related to the erroneous implementation of the heat transfer correlation for reflooding (bottom up). The quench model in the TRACG code has been corrected and the corrected code will be used in all future TRACG LOCA applications.

Summary of Qualification Relevant to BWRs/3-6 LOCA Evaluations

As part of the error assessment, qualification calculations related to the quench model for bottom reflooding were updated and the impact of the quench model on predicted PCTs quantified as indicated in the RAI-49 response for the case of a rising quench front like that observed in a reflooding situation. Use of the TRACG quench model was shown in MFN 13-085 (Reference [R104- 18]) to result in calculated cladding temperature responses that compare well to the measured temperature responses from LOCA Integral System Tests (IST) where reflood quenches were experienced. Key selected results from Reference [R104- 18] for LOCA scenarios are replicated in this document. The comparison to Halden tests that were added for ATWSI applications at high pressure are not included because for LOCA scenarios where fluid inventory and pressure are substantially lower, the comparisons with LOCA-like IST data are more relevant.

Cases were selected for tests performed at facilities that had previously been evaluated in the TRACG Qualification LTR (Reference [R104- 9]) except for THTF test 3.03.6AR which was specifically added at the request of the NRC because it had also been evaluated using TRACE. Selected cases are those where the test data temperature traces indicate a quench since these are the cases where the impact of the TRACG quench modeling are expected to be greatest. The tests evaluated in this response are: Thermal Hydraulic Test Facility (THTF) transient blow down tests 3.03.6AR, 3.06.6B, and 3.08.6C (References [R104- 19], [R104- 20]); Two-Loop Test Apparatus (TLTA) test 6423 (Reference [R104- 21]); ROSA-III test 912 (Reference [R104- 22]); and ROSA-III test 926 (Reference [R104- 23]). Relevant details for the re-evaluations presented here are summarized in Table R104-3. All the TRACG calculations were executed using the Shumway Tmin correlation with the void term disabled and the cladding material appropriate for the test as indicated in Table R104-3.

The temperatures presented in Table R104-3 show that generally the maximum temperature calculated by TRACG [[

]] for these LOCA-like cases the maximum

temperature is reached and begins to decrease based on precursory steam cooling that exists prior to when the quench occurs. The LOCA scenarios are unlike the ATWSi scenario because for LOCA the cladding has a longer heatup time at a much lower heat flux in a fluid environment where there is very little liquid water. The ATWSi scenario with power and flow oscillations near the operating reactor pressure is much better represented by the Halden test cases where the reactor remains at power, flow is reduced to produce the boiling transition and is later increased after the dryout to simulate the flow surge, which causes the return to nucleate boiling.

Table R104-3 : Test Data and TRACG Comparison Summary for LOCA-like Scenarios

Test	Clad Material	Maximum Temperature[1] (K)				Quench Velocity[3] (m/s)		Estimated Pressure (MPa) at Time of Quench
		Test Data	TRACG Quench Model OFF	TRACG Quench Model ON	Elev-ation[2] (m)	Avg. along rod	Last Second Before Quench	
THTF 3.03.6AR	Stainless Steel	949	[[		3.6	0.08	0.43	5.6
THTF 3.06.6B	Stainless Steel	1135			3.6	0.11	0.32	5.8
THTF 3.08.6C	Stainless Steel	1204			2.4	0.10	0.07	6.6
TLTA 6423	Inconel	802			2.0	0.01	0.05	0.60
ROSA-III 912	Inconel	839			0.94, 1.11	0.02	0.15	1.4
ROSA-III 926	Inconel	784		]]	0.94	0.01	0.07	0.40

[1]The *Maximum Temperature* corresponds to the peak value for the specific rod and location that is being compared.

[2]The elevation indicates where the maximum temperature was taken for the test data and TRACG. The maximum temperature from the node plotted for the respective test and elevation is used. For ROSA-III 912, the TRACG calculated temperature peak occurs for the node at 1.11m so it is the temperature trace at that elevation that is tabulated and plotted.

[3]The *Quench Velocity* was calculated by dividing the distance the quench front traveled by the elapsed time to travel that distance based on the TRACG indicated position of the quench front with time.

Table R104-3 shows that for THTF tests 3.03.6AR and 3.06.6B the calculated quench velocity over the last second before the quench at the thermocouple (T/C) elevations are respectively 0.43 and 0.32 m/s (16.9 and 12.6 inch/s). The ATWSi power/flow oscillations occur near the normal operating pressure of a BWR whereas for the LOCA-like test cases the quench occurs for a range of lower pressures as indicated in the rightmost column of Table R104-3.

Calculated TRACG temperature traces with time are compared to the test data in Figure R104-5 through Figure R104-10. The red curves labeled "TRACG Nominal" in these figures are from calculations where the quench model was turned OFF. The blue curves labeled "TRACG Quench" are with the quench model turned ON. The green and turquoise curves show the measured data. For these LOCA scenarios the quench front movement is limited by the rate of liquid water addition rather than the inability to return to nucleate boiling. Steam produced lower in the bundle serves to reduce measured temperatures at the higher elevations before the quench front propagates to the maximum measured temperature elevation. It is this precursory cooling process that is the

reason both the measured and calculated temperature traces are trending downward even before quenching occurs. Quench is suggested at the *shoulder* in the measured temperature trace where the temperature suddenly drops.

It is not always possible from the measured temperature traces to distinguish a temperature drop due to quenching and a drop due to an improvement in the heat transfer mode that results when the surface temperature is reduced below the minimum stable film temperature (Tmin). The need to make this distinction is not essential because the TRACG quench and Tmin models work together. The Tmin model defines the maximum surface temperature for which return to nucleate boiling can occur if there is sufficient liquid. When the surface temperature ahead of the quench front is above Tmin, the quench model has a higher relative importance because it provides for heat removal via axial conduction to liquid near the saturation temperature that exists below the quench front. On the other hand, if the surface temperature decreases below Tmin above the quench front then a higher heat transfer coefficient is calculated above the quench front and the axial temperature profile and thus the quench heat removal mechanism are decreased. The TRACG Quench calculations presented in Figure R104-5 through Figure R104-10 demonstrate that the TRACG quench and Tmin models are working well together in matching the quench temperature data. For example, consider the results in Figure R104-6 for THTF test 3.06.6B. For pressures between 5 and 6 MPa the Shumway correlation predicts a Tmin value of about 770 K for stainless steel for low flows and no void enhancement. Graphically it can be seen [[

]]

For comparison with the TRACG calculations and the test data, the TRACE calculated results are depicted by the purple curves in Figure R104-5, Figure R104-6, and Figure R104-7. As stated previously, the Groeneveld-Stewart Tmin correlation (derived from Inconel data) is used in TRACE to predict a Tmin value around 685 K at 5 MPa. This value is about 90 K lower than the Shumway prediction for stainless steel at 5 MPa. The impact of the lower value for Tmin is most apparent in the purple curves on the left side of Figure R104-6 and the right side of Figure R104-7. Primarily because of the lower value for Tmin, TRACE predicts a quench temperature that is lower than the data by at least 50 K.

In all cases of reflood quenching from below, both the measured and calculated results indicate quenching occurs after the temperature has peaked and has begun to decrease. In other words, the quenching phenomena for reflood scenarios with a rising quench front like those occurring in BWRs/3-6 is of “low” importance for determining the peak clad temperature (PCT) because precursory cooling has already caused the cladding temperature to start decreasing before the quench front rises to the PCT location. The differences in the calculated TRACG temperatures

with the quench model off (red curve) and with the quench model on (blue) curve are insignificant as shown in Figure R104-5 through Figure R104-10. This is the main reason that C21 for quench is ranked as having "low" importance in LTR Table 4.2-1 for all phases of BWRs/3-6 LOCAs where the dominant quenching mechanism is due to bottom reflooding. As explained in the response to RAI-51: "For jet pump plants, rewet occurs after reflood and the temperature has turned around and starts to come down. The uncertainty in the rewet has therefore no impact on the PCT. Likewise the impact on the fuel clad oxidization for jet pump plants is also minimal as the PCT is relatively low and the duration of refill/reflood phase is short."

Summary of Qualification Relevant to BWR/2 LOCA Evaluations

For larger breaks in a BWR/2, core reflooding is not possible, quenching as a result of core spray occurs from a falling quench front which does have an impact on the calculated PCT and ECO values. This is the reason that the bias and uncertainty for the quench front modeling were determined from falling quench front data as explained in the response to RAI-49. The relevant qualification of the model comes from the Core Spray Heat Transfer (CSHT) tests.

Uncertainty in the quench model is not modeled as part of the approved SAFER/CORECOOL application so in that sense the TRACG implementation is more rigorous. As indicated in Section 5.1.3.27 of the LTR and the response to RAI 49, the bias and uncertainty in the quench model are conservatively established as respectively, [[ ]]. In the proposed TRACG LOCA methodology the bias is removed and uncertainty is sampled as part of the BEPU process. Accounting for the non-conservative bias and twice the uncertainty results in a PIRT83 value of [[ ]].

The modeling of quench bias and uncertainty for a falling film has been quantified by comparisons to CSHT data since for these tests quenching is due to a falling film like in a BWR/2. Monte Carlo analyses of select CSHT tests (using 59 statistical trials) were provided in Section 7.4.5 of the TRACG LOCA LTR to show how treatment of the uncertainties impacts the comparison with the data. The text and figures in Section 7.4.5 have been updated and augmented in the response to RAIs 82 and 92.

Studsvik Core Spray Heat Transfer Tests

Studsvik (Reference [R104- 24]) core spray heat transfer tests 111, 133, and 137 were analyzed in response to RAI-82. These three particular tests were selected because they had the highest measured temperatures. These evaluations augment CSHT tests previously evaluated in the TRACG LOCA LTR and in Section 3.2.2 of the TRACG Qualification LTR (Reference [R104- 9]). The maximum of the calculated temperatures from the locations where there were measurements is compared to the maximum of the measured Studsvik data for these locations in Figures R82-3, R82-4, and R82-5 of RAI-82. The comparisons show that on average TRACG tends to conservatively over predictive the measured data but still within the uncertainty band of the 59 Monte Carlo simulations. Data collection for Studsvik tests 111, 133, and 137 was terminated prior to quench.

Fortunately, data collection for Studsvik test 123 extended long enough to include the quench. TRACG evaluations were also performed for test 123 in response to RAI-82 even though test 123

produced a lower measured PCT than tests 111, 133, 137. Studsvik test 123 was specifically designed as a bottom-vented test so it is more representative for a large LOCA in a BWR/2. The TRACG simulations for this test were intended to show the negligible impact of noncondensable gases (NCG) but the results in Figure 82-2 of the RAI response also show that the maximum of the nominal calculated temperatures is conservatively high compared to the corresponding maximum of the measurements. TRACG also conservatively predicts a later quench than seen in the experimental data. For convenience, Figure 82-2 of the RAI response is replicated here as Figure R104-11.

GE Core Spray Heat Transfer (CSHT) Tests

The CSHT tests utilized a full-scale simulated 8x8 BWR bundle consisting of 63 electrically-heat *fuel* rods and one central un-heated water rod. The test facility, test descriptions, the TRACG modeling, and the comparison of calculated and measured results are all given in Section 3.2 2 of the TRACG Qualification LTR (Reference [R104- 9]). Essential elements are repeated here for convenience.

There are total of six transient CSHT tests documented in Section 3.2 2 of the TRACG Qualification LTR (Reference [R104- 9]). Figures 3.2-13 through 3.2-18 in Reference [R104- 9] show comparisons of the TRACG calculated temperatures from all rod groups (RGs) where test data was available for each of the six tests. All calculational setups used the rod grouping shown in Figure 3.2-8 of Reference [R104- 9] together with the test-specific rod peaking factors shown in the table below the figure. For convenient referral during the discussion that follows, the figure and table are replicated here as Figure R104-12.

For three of the CSHT tests (111, 120, and 121) the data was recorded long enough to show the full quench. Test 111 has the highest measured initial PCT from tests 111, 120, and 121; therefore, test 111 was selected in the original TRACG LOCA LTR for assessing the calculated rod PCTs and rod quenching characteristics. Updated TRACG Monte Carlo calculations (using 59 trials) are presented in RAI-92 for CSHT tests 111, 112, and 110. Calculations for test 112 were also updated in RAI-92 because test 112 has the highest initial rod PCT, among all six tests (Reference [R104- 9] Table 3.2-3). Unfortunately, data collection for test 112 ended at 500 seconds (prior to the quench) so comparison of this test for quenching with TRACG is not possible.

The 59 Monte Carlo simulations for each of CSHT tests 110, 111, and 112 as documented in the RAI-92 response applied the same TRACG model uncertainties as established in the LTR for plant applications. Note that the statistical analyses for these CSHT tests only considered TRACG model parameter uncertainties and the uncertainties in the measured core spray flow to the bundle and in the spray liquid temperature. Other uncertainties associated with heater rod material properties, power distribution, initial conditions, and heat transfer due to spray on the outside of the channel were not considered. It is expected that consideration of these additional uncertainties and increasing the number of trials from 59 to at least 124 (as now required for plant calculations) would expand the span in calculated temperatures and cause them to cover all the measured values. As it was, a few of the measured temperature values for RGs 2 and 4 from tests 111 and 112 extend slightly outside the span of the Monte Carlo calculations. Calculated results for the hot rod group

(RG=10) were not previously shown in the RAI-92 response but are included later in this discussion in Figure R104-18.

As noted in the RAI-92 response, TRACG calculated nominal peak temperatures on average are 13 K higher than the data when considering all six CSHT tests and all the rod groups identified in Table 3.2-4 of [R104- 9] where test data was available. Nominally considering these rod groups, the peak temperatures for tests 111 and 112 are slightly under predicted whereas the peak temperatures are over predicted for tests 113, 120, and 121.

For CSHT test 110 the nominal calculations for the peak temperatures for all rod groups are predicted well within the span of {-5.1, 15.0} relative to the data. For purposes of demonstrating the coverage of the TRACG model uncertainties, CSHT test 110 is a good choice because any biases associated with modeling the power differences between rod groups appear to have been minimized. (Note that such biases are not relevant in the plant applications where the limiting LHGR values are prescribed to account for a conservative local peaking factor both radially and axially within the fuel bundles.) Calculated 59-trial Monte Carlo results for rod groups 2, 3, 4, 6 in CSHT test 110 are shown in the response for RAI-92. The measured temperature data shows a drop of about 50 K around 1000 seconds for rod groups 2 and 4 (see Figures R92-10 and R92-12 in RAI-92). A short time later the lower extremes of the TRACG Monte Carlo calculations for these rod groups also show a drop which suggests that for some scenarios the quench has begun in the lower power rod groups. The recorded data was terminated before full quench was achieved; however, TRACG simulations that extend out to 3000 seconds for test 110 reveal that TRACG generally is predicting the quench slightly later than the data suggests so that TRACG results are conservative with respect to cladding temperature and accumulated oxidation.

Test 111 is the best CSHT test for assessing the timing of the quench predicted in the TRACG calculations because the test data extends past the time of full quench (defined as time when cladding temperature decreases within 10 K of the fluid temperature). Calculated results for rod groups 2, 3, 4, 6, and 9 are shown in Figures R92-1 through R92-5 in the response for RAI-92. These figures are replicated here as Figure R104-13 through Figure R104-17 for convenient referral during the discussion that follows. The calculated results for the hot rod group 10 are shown here in Figure R104-18 although they were not previously provided in the response to RAI-92.

Comparisons of the calculated temperature responses versus data for each rod group (RG) is informative because it demonstrates how the quench model has been implemented within the TRACG CHAN component. As explained in the description of the quench model, each surface is treated individually where a surface corresponds to a fuel rod group, water rod group, or channel box. The unpowered surfaces for channel box and water rod quench first generally followed by the powered corner rod then powered interior rods. Because of differences in radiative view factors, the expectation is that the powered RGs will quench in order starting from the corner and moving inward. The rod peaking factors play a role in determining the order of quenching but if they are reasonably close together the position of the rod within the bundle will be more important especially for higher temperatures where the radiative heat transfer component is more important. All rods within the one-dimensional CHAN component experience the same axial distribution of

hydraulic conditions; however, the radiative view factors and rod heat conduction solution is performed individually for each RG. TRACG also applies a conservative bias for convective heat transfer to vapor for interior rods in a bundle.

For the surfaces where thermocouples (TCs) were present there are comparisons between the calculated and measured temperatures. The TC data for each RG that is plotted in the figures is taken as the maximum value from all TCs for rods assigned to that RG since this will present the greatest challenge for the uncertainty in modeling to cover. These data values for CSHT test 111 are indicated by the pink squares in Figure R104-13 through Figure R104-18.

Let us consider the comparisons between calculations and data for the RGs starting from the outside corner and working diagonally inward (see Figure R104-12) in what is the expected approximate order of quench; i.e., RGs 9, 6, 4, 3, 2, and 10.

[[

]]

[[

]] Overall, the TRACG quench model is conservatively providing a somewhat later quench that the data.

[[

]] Notice how this nominal slope from the calculation compares favorably with the slope in the data points. This excellent agreement suggests an accurate value for the overall heat transfer coefficient to vapor prior to quench.

Figure R104-18 shows calculations for RG 10 which has been designated in the TRACG input model as the “hot rod group” (HRG). These comparisons were not previously shown in response

to RAI-92 although they probably should have been. [[

]]

As explained in Section 6.6.10 of Reference [R104- 3] on the film boiling heat transfer at high void fraction, [[

]]

Additional details for the hot rod model are provided in Section 7.5.7 of Reference [R104- 3]. Relevant portions have been summarized here. Experience from the qualification has shown that TRACG calculates the average fuel rod temperatures very well based on the average hydraulic conditions. Cross-sectional variations in the hydraulic conditions, however, can lead to local variations in heat transfer and fuel temperatures that are different from the averages. This is particularly the case for high void fractions where the flow is in the annular flow regime and where the rods are in film boiling heat transfer. This is typically only important for the reflood phase of a LOCA prior to the quenching of the fuel rods. The hot rod model also accounts for this phenomenon. [[

]]

[[

]]

[[

]]

The appropriateness of the model parameter uncertainties associated with quench and the statistical process used to combine them has been demonstrated by applying the BEPU approach to Studsvik and GE CSHT integral system tests. [[

]] The calculations demonstrate that the quench model and hot rod model perform as designed. In general, the quench times predicted by the TRACG modeling is delayed relative to the CSHT data which means that TRACG will conservatively over estimate the amount of oxide that will accumulate prior to full quench when applied in plant LOCA applications.

Discussion of Table R104-4 Sensitivity Studies

To respond to the specific NRC request in this document, sensitivity studies have been performed to justify the current treatment of bias and uncertainty for both the **M**odified **S**humway (MS) correlation for minimum stable film temperature (Tmin) and the quench model. ALL sensitivity studies have been performed using 181 statistical trials and the limiting case for the NMP1 BWR/2 LOCA analysis. Use of the NMP1 BWR/2 calculations for the sensitivity studies is the most appropriate because the time in boiling transition for a BWR/2 is substantially longer than for BWRs/3-6 LOCA evaluations because for the limiting BWR/2 LOCA scenario only core spray is available to cool the core. Consequently, rewetting occurs much later and the impact of any process that delays rewetting has the largest impact on oxide accumulation. By comparison, the cores in jet pump BWRs/3-6 can be re-flooded by the ECCS systems at least to the top of the jet pump diffusers within a comparatively shorter period of time so that total oxide accumulation remains much less than the imposed regulatory limit of 13% for maximum local cladding oxidation (MLO). It is also true that BWR/2 LOCA calculations tend to provide a higher calculated peak

clad temperature (PCT) relative to BWRs/3-6 evaluated for the same linear heat generation rate (LHGR).

During the teleconference on August 16, 2016 the NRC expressed concern that by biasing Tmin the maximum local oxide from the highest rank trial could challenge the 13% acceptance criteria. To quantify the impact of adding an intentional bias on Tmin, the MLO values for the highest rank were provided for 59 trials, 124 trials, and 181 trials as part of the follow-up email. It is not surprising that imposing additional conservative bias on Tmin will increase the mean MLO and may also increase the highest rank values as well. It is not GEH's intention to suggest an alternative approach that biases Tmin rather than de-biasing it and sampling since that would be a deviation from the BEPU approach that already appropriately accounts for bias and uncertainty in Tmin.

Results presented in prior communications have been superseded. The design limitations for the NMP1 core have been re-specified to provide slightly more margin to the imposed 13% oxide limitation. Specifically, the LHGR curve used for LOCA analyses (hence core design) has been modified slightly as shown in Figure R104-19. [[

]] All values presented below in Table R104-4 reflect the revised LHGR design curve for NMP2. The effect of the slight change in LHGR curve is illustrated by noting that previously the highest rank MLO value out of 181 trials was reported as [[ ]] compared to the updated value of [[ ]] shown in cell [C11a] of Table R104-4.

Column and row numbers are used in Table R104-4 to facilitate discussion of the results. In this discussion particular cells are referenced as [a#] where "a" is the letter of the column and "#" is the row number in Table R104-4. Columns A and B in the table describe the quantities for which values are presented in columns C through F. The base values presented in column C are those for the BEPU sampling process described in the LTR. According to the TRACG LOCA methodology under review, the LOCA licensing basis would be defined from the values in column C. The other results in columns D through F are presented in response to this RAI request to show the sensitivity of the key results in response to the modeling of bias and uncertainty in Tmin and quench.

Table R104-4 also provides additional details for the specific trials that produce the three highest rank values for PCT and MLO. [[

]]

For the Tmin sensitivity results shown in column D [[

]]

For the Tmin sensitivity results shown in column D, the impact on the mean of the maximum local oxide (MLO) is [[

]]

The results for the quench model sensitivity studies have not been previously presented. The quench study results like the results from the Tmin studies are presented Table R104-4 and they

also reflect the revised LHGR design curve for NMP2. Consequently, the base BEPU values in column C used as a reference for the Tmin studies also are applicable as a basis for the quench studies. As explained previously, [[

]] This approach for assessing the quench model is parallel to the process used to assess the Tmin model.

The sensitivity results for quench are shown in column E of Table R104-4. [[

]]

The mean MLO for the quench sensitivity [[

]]

There are some important observations regarding the quench sensitivity results in column E of Table R104-4. [[

]]

The PCT and MLO move in opposite directions when the quench rate is reduced (column E results). This is evidence that the presumed bi-variant relationship between PCT and MLO changes is complicated and likely to depend on the transient scenario. Repeatedly GEH has stated that the PCT and MLO values occur in different channels at different axial locations within the core. The maximum values of PCT and MLO also occur at different points in time and usually for a different trial as shown by the trial numbers that provided the max# value shown in Table R104-4 in the row below the max# value.

The proposed BEPU approach provides the best solution because it does not distort the transient scenario by increasing conservatism relative to one acceptance criterion at the expense of decreased conservatism for another acceptance criterion. Consider the base BEPU numbers in Column C of Table R104-4. [[

]]

Conclusions

The requested sensitivity studies are summarized in Table R104-4. The MLO values in the lower half of the table indicate the expected increases corresponding to imposition of additional conservatism in calculated MLO values associated with the modeling of Tmin and quench. The PCT values in the upper half of the table generally indicate that imposing conservatism in modeling of Tmin has only a small impact whereas imposing conservatism on the quench modeling reduces the mean and upper bound PCTs. The imposition of additional conservatism is not warranted because the BEPU modeling described in the TRACG LOCA LTR already accounts for bias and uncertainty in the modeling of Tmin and quench in a way that satisfies the regulatory requirements and guidance. The current BEPU modeling of bias and uncertainty for Tmin and quench are justified based on good comparisons between the relevant qualification calculations and the experimental data.

Table R104-4 Sensitivity Results for Tmin and Quench

[[

]]

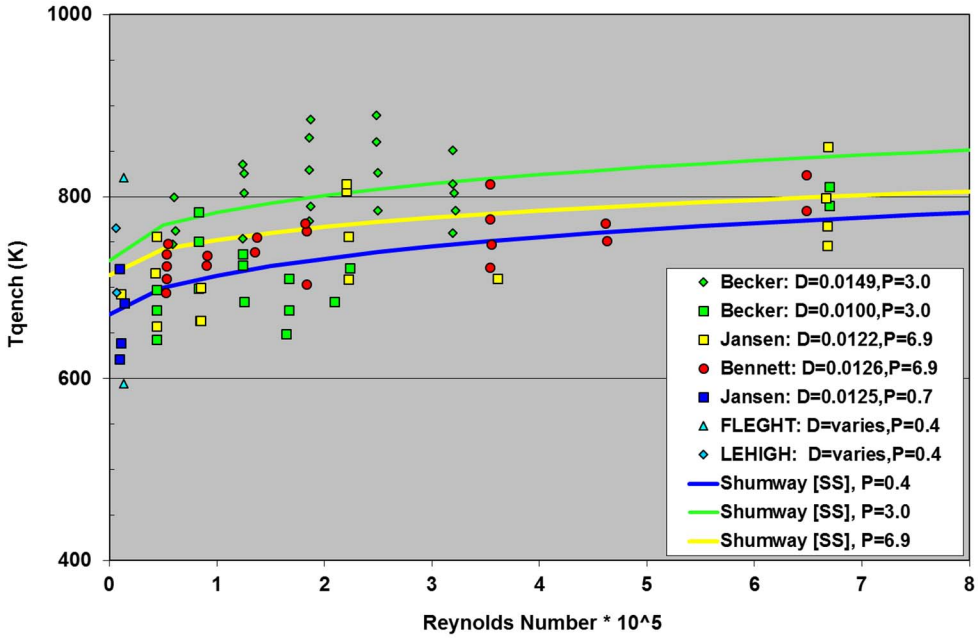

Figure R104-1 Shumway Correlation versus his Stainless Steel Data {Fig. 1 in [R104- 2]}

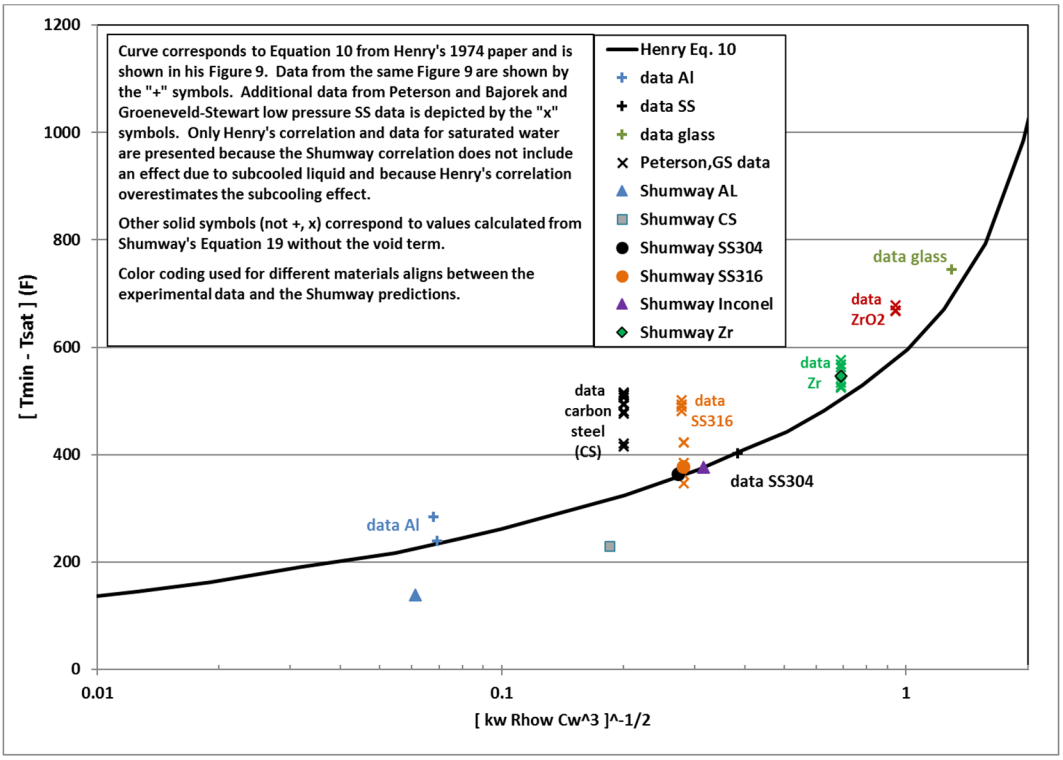

Figure R104-2 Shumway Correlation for Different Materials {Fig. 4 in [R104- 2]}

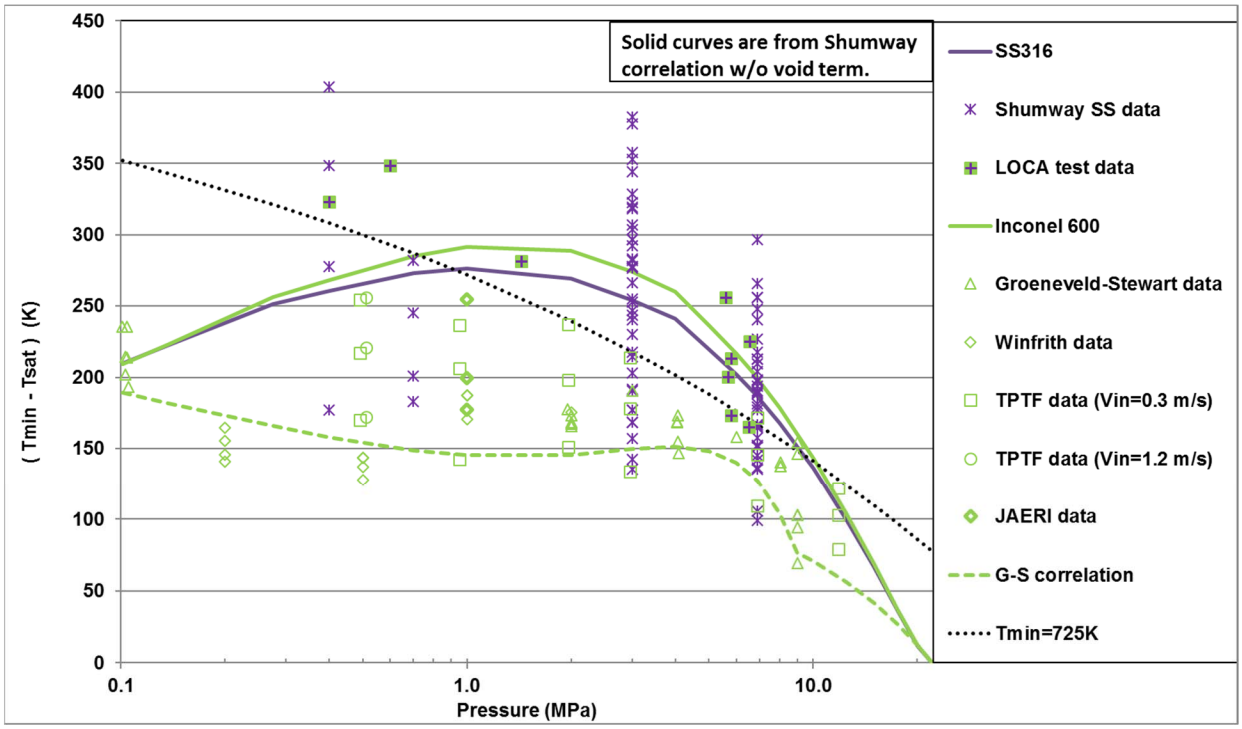

Figure R104-3 Shumway Compared to SS and Inconel Data {Fig. 5 in [R104- 2]}

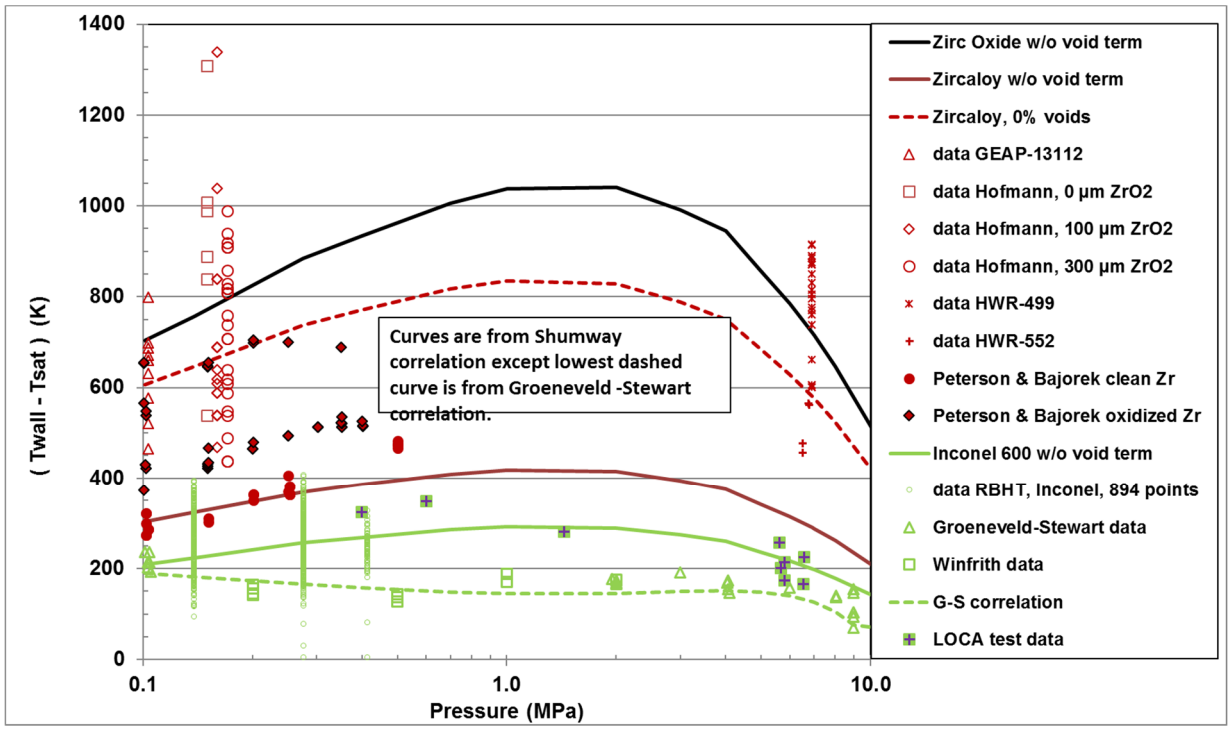

Figure R104-4 Shumway Compared to Inconel and Zircaloy Data {Fig. 6 in [R104- 2]}

[[

]]

Figure R104-5 Temperature Comparison for THTF Test 3.03.6AR {Fig. 8 in [R104- 18]}

[[

]]

Figure R104-6 Temperature Comparison for THT Test 3.06.6B {Fig. 9 in [R104- 18]}

[[

]]

Figure R104-7 Temperature Comparison for THT Test 3.08.6C {Fig. 10 in [R104- 18]}

[[

]]

Figure R104-8 Temperature Comparison for TLTA Test 6423 {Fig. 11 in [R104- 18]}

[[

]]

Figure R104-9 Temperature Comparison for ROSA-III Test 912 {Fig. 12 in [R104- 18]}

[[

]]

Figure R104-10 Temperature Comparison for ROSA-III Test 926 {Fig. 13 in [R104- 18]}

[[

]]

Figure R104-11 Studsvik CSHT Test 123 – Cladding Temperatures {Fig. R82-2}

[[

]]

Figure R104-12 Rod Grouping for CSHT Simulations {Fig. 3.2-8 of [R104- 9]}

[[

]]

Figure R104-13 CSHT Test 111, Rod Group 2 {Fig. R92-1}

[[

]]

Figure R104-14 CSHT Test 111, Rod Group 3 {Fig. R92-2}

[[

]]

Figure R104-15 CSHT Test 111, Rod Group 4 {Fig. R92-3}

[[

]]

Figure R104-16 CSHT Test 111, Rod Group 6 {Fig. R92-4}

[[

]]

Figure R104-17 CSHT Test 111, Rod Group 9 {Fig. R92-5}

[[

]]

Figure R104-18 CSHT Test 111, Rod Group 10 {not in R92}

[[

]]

Figure R104-19 Revised LHGR Design Curve for NMP1

REFERENCES

[R104- 1] Letter, J. F. Harrison (GEH) to Document Control Desk (NRC), "Final Presentation for ACRS Thermal-Hydraulic Phenomena Subcommittee Meeting on September 21, 2015 and Final Presentation and Requested Information for NRC Audit Related to the Peach Bottom Units 2 and 3 License Amendment Request for MELLLA+, August 31, 2015 to September 2, 2015," MFN 15-078, September 25, 2015.

[R104- 2] Letter, J. F. Harrison (GEH) to U. S. Nuclear Regulatory Commission, "Use of the Shumway Tmin Correlation with Zircaloy for TRACG Analyses," MFN 13-073, September 9, 2013.

[R104- 3] J. G. M. Andersen, et al., "TRACG Model Description," NEDE-32176P, Revision 4, January 2008.

[R104- 4] R.W. Shumway, "TRACG-BWR Heat Transfer: Assessment of Tmin", EGG-RST-6781, January 1985.

[R104- 5] Henry, R.E., "A Correlation for the Minimum Film Boiling Temperature", Heat Transfer Reasearch and Design, AIChE Symposium, Series 70, No. 138, 1974, pp. 81-90.

[R104- 6] Peterson, L.J. and S.M. Bajorek; *Experimental Investigation of Minimum Film Boiling Temperature for Vertical Cylinders at Elevated Pressure*; Proceedings of ICONE10 10th; Arlington, VA; April 14-18, 2002.

[R104- 7] J.C. Stewart and D.C. Groeneveld, "Low-Quality and Subcooled Film Boiling of Water at Elevated Pressures," *Nuclear Engineering Design*, 67, 1981, pp. 259-272.

[R104- 8] *TRACE V5.0 Theory Manual: Field Equations, Solution Methods, and Physical Models*; citations used here is for version last updated 2012-05-07; following link may be more recent: http://www.nrc.gov/docs/ML1200/ML120060218.pdf

[R104- 9] *TRACG Qualification*, NEDE-32177P, Revision 3, August 2007.

[R104- 10] Hochreiter, L.E. et al., *RBHT Reflood Heat Transfer Experiments Data and Analysis*, NUREG/CR-6980, April 2012.

[R104- 11] Duncan, J.D. and J.E. Leonard, *Thermal Response and Cladding Performance of an Internally Pressurized Zircaloy-Clad Simulated BWR Fuel Bundled Cooled by Spray Under Loss-of-Coolant Conditions,* GEAP-13112, April 1971.

[R104- 12] Hofmann, P. et al., Quench Behavior of Zircaloy Fuel Rod Cladding Tubes: Small-Scale Experiments and Modeling of the Quench Phenomena, FZKA 6208, Forschungszentrum Karlsruhe, March 1999.

[R104- 13] McGrath, M., *Minutes of the Fourth Workshop on Dry-out Fuel Behaviour Tests (IFA-613)*, HWR-499, OECD Halden Reactor Project, April 1997.

[R104- 14] Ianiri, R., *The Third Dryout Fuel Behaviour Test Series in IFA-613*, HWR-552, OECD Halden Reactor Project, February 1998.

[R104- 15] Safety Evaluation by the Office of Nuclear Reactor Regulation Relating to General Electric Company Licensing Topical Report NEDE-30996P Volume 1 "SAFER Model for Evaluation of Loss-Of-Coolant Accidents for Jet Pump and Non-Jet Pump Plants".

[R104- 16] Letter G.C. Lainas (NRC) to H.C. Pfefferlen (GE), "Review of NEDE-~~2~~30996(P), 'SAFER Mdels for Evaluation of Loss-of-Coolant Accident for Jet Pump and Non-Jet Pump Plants, Volumes I and II'," HCP-017-087, February 19, 1987.

[R104- 17] S.K.W. Yu, P.R. Farmer, and M.W. Coney, *Methods and Correlations for the Prediction of Quenching Rates on Hot Surfaces*, International Journal of Multiphase Flow, 3, 1977, pp. 415-443.

[R104- 18] Letter J.F. Harrison (GEH) to Document Control Desk (NRC), "Update TRACG Quench Front Model Description and Qualification", MFN 13-085, October 15, 2013.

[R104- 19] *An Analysis of Transient Film Boiling of High-Pressure Water in a Rod Bundle*, NUREG/CR-2469, March 1982.

[R104- 20] TRACE V5.0 Assessment Manual, Appendix B: Separate Effects Tests, http://pbadupws.nrc.gov/docs/ML1200/ML120060191.pdf

[R104- 21] BWR Large Break Simulation Tests – BWR Blowdown/Emergency Core Cooling Program, GEAP-24962, NUREG/CR-2229, March 1981.

[R104- 22] Experiment Data of ROSA-III Integral Test Run 912, JAERI-M 82-010, January 1982.

[R104- 23] ROSA-III 200% Double-ended Break Integral Test RUN 926, JAERI-M 84-008, February 1984.

[R104- 24] Studsvik Report, "BWR Emergency Core Cooling Investigations – Spray Cooling Heat Transfer Experiment in a Full Scale BWR Bund Mock-up", STUDSVIK/E4-78/64, October 4, 1978.